CONF-7809129--1

MASTER

SLAC-PUB-2208
October 1978
(T/E)

EXPERIMENTAL TEST OF EXCHANGE DEGENERACY IN HYPERCHARGE EXCHANGE REACTIONS*

K. C. Moffeit
Stanford Linear Accelerator Center
Stanford University, Stanford, California 94305
U.S.A.

Introduction

The two pairs of line-reversed reactions

$$\pi^+ p \to K^+ \Sigma^+ \quad (1)$$

$$K^- p \to \pi^- \Sigma^+ \quad (2)$$

and

$$\pi^+ p \to K^+ Y^{*+}(1385) \quad (3)$$

$$K^- p \to \pi^- Y^{*+}(1385) \quad (4)$$

provide experimental test of exchange degeneracy in hypercharge exchange reactions. The reactions are expected to be dominated by vector and tensor K^* exchanges. Exchange Degeneracy (EXD) of these trajectories implies equal cross sections for reactions (1) and (2) [(3) and (4)] at the same value of the four-momentum transfer, t. The polarization of the final state hyperon should be either zero (strong EXD) or, if different from zero, it should have equal magnitude and opposite sign (weak EXD) in line-reversed reactions.[1] In order to see these Exchange Degeneracy predictions, we write the differential cross section and

* Work supported by the Department of Energy under Contract No. EY-76-C-03-0515.

(Invited talk presented at the Seoul Symposium on Elementary Particle Physics, Seoul National University, Seoul, Korea, September 1-5, 1978.)

polarization in terms of the Regge amplitudes

$$\frac{d\sigma}{dt} = |A_+|^2 + |A_-|^2$$

$$P\frac{d\sigma}{dt} = -2\,\mathrm{Im}\,(A_+ A_-^*) \quad (5)$$

where + (−) refer to s-channel helicity non-flip (flip) amplitudes. For the line-reversed reactions

$$A_\pm(\pi^+ p \to K^+ Y^+) = (-K^* + K^{**})_\pm$$

$$A_\pm(K^- p \to \pi^- Y^+) = (K^* + K^{**})_\pm \quad (6)$$

where Y refers to either the Σ or $Y^*(1385)$ and

$$K^* = \beta_{K^*}(1 - e^{-i\pi\alpha_{K^*}})\left(\frac{s}{s_0}\right)^{\alpha_{K^*}}$$

$$K^{**} = \beta_{K^{**}}(1 + e^{-i\pi\alpha_{K^{**}}})\left(\frac{s}{s_0}\right)^{\alpha_{K^{**}}} \quad (7)$$

Here β and α represent the residue and trajectory for the vector K^* and tensor K^{**} Regge poles. The weak exchange degeneracy hypothesis assumes the K^* and K^{**} trajectories are equal ($\alpha_{K^*} = \alpha_{K^{**}}$), but the residues are not equal ($\beta_{K^*} \neq \beta_{K^{**}}$). Complete degeneracy of the trajectories is assumed in the strong exchange degeneracy hypothesis with α and β equal for the vector and tensor K^* exchange. These assumptions lead to the predictions discussed above.

Experimental Technique

Recent tests of EXD predictions have been done at higher energies and with high statistics. The line-reversed reactions are also studied in the same experimental setup. These experiments have been done by

two basic experimental techniques: 1) missing-mass method and 2) the target sensitive method using a hybrid bubble chamber.

Berglund et al. use the missing-mass method to obtain their 7 and 10.1 GeV/c data at CERN.[2] The ANL-FNAL-SLAC collaboration[3] also use the missing mass technique to study the π^+p reactions at 35, 70, and 140 GeV/c and K^-p at 70 GeV/c; only their 70 GeV/c π^+p data is available at this time.

The experimental setup for the missing-mass method consist of measuring only the beam $\pi^+(K^-)$ and the forward $K^+(\pi^-)$. The mass of the particles are identified by the signals from Čerenkov counters in the beam line and forward spectrometer. Figure 1 shows the missing-mass-squared distribution for π^+ in the beam and K^+ in the spectrometer, summed over all 70 GeV/c data from the experiment of Arenton et al.[3] Since all exclusive reactions are obtained at the same time, the experimenters obtain the cross sections for ρ, $Y^*(1385)$, etc. by fitting to the missing-mass distribution in various momentum-transfer regions.

The other technique uses the hybrid bubble chamber at SLAC.[4] The facility, shown in Fig. 2, consists of a rapid cycling bubble chamber followed by an electronic system (proportional wire chambers, Čerenkov, and scintillator hodoscopes). The chamber expands at its maximum rate (typically 15pps) and when an event of interest is recorded in the electronic system, the lights of the chamber are flashed and the picture is taken. Since it takes three milliseconds for the bubbles in the chamber to grow large enough to be photographed, the decision as to whether or not to flash the lights can be made with the aid of a small on-line computer. The 4π detection of charged tracks in the bubble

chamber allows a cleaner separation of reactions by topology and kinematic fitting than in missing-mass techniques. The invariant mass distribution of the $\Lambda\pi^+$ system from both the π^+ and K^- induced reactions show a prominent peak due to the $Y^*(1385)$ production as seen in Fig. 3. These distributions show the ability of the bubble chamber to isolate reactions and thereby reduce background.

History of Exchange Degeneracy in Hypercharge Exchange Reactions

Previous measurements of reactions (1) to (4) have mostly resulted from experiments done by different groups using different techniques,[5,6] thus making comparisons difficult to interpret. The early experimental test of Exchange Degeneracy occured at lower energies and the data showed large violation of EXD predictions, viz, $d\sigma/dt\ (\pi^+p) < d\sigma/dt\ (K^-p)$, and the Σ^+ polarizations did not reflect about zero.[6] However, a good description of the lower-energy $d\sigma/dt$ and polarization measurements for both reactions (1) and (2) was made from the model of Navelet and Stevens[7] using an effective cut parametrization in addition to the $K^*(890)$ and $K^{**}(1420)$ pole terms. Their model predicted significant violations of exchange degeneracy in the energy region of 10 to 12 GeV/c and even at 70 GeV/c.

Recent Results for the Reactions $\pi^+p \to K^+\Sigma^+$ and $K^-p \to \pi^-\Sigma^+$

Differential cross sections from the SLAC-Imperial College experiment[8] for these reactions to $|t| = 1\ (GeV/c)^2$ are shown in Figs. 4(a) and 4(b). They confirm earlier results in showing a simple exponential behavior for $|t| < 0.4\ (GeV/c)^2$. There is no evidence for a turnover in the forward direction, indicating dominance of the non-flip

helicity amplitude, at least at low momentum transfer. At both energies the π^+ induced reaction slopes are steeper than for the K^- reactions, although the difference is less at the higher momentum. Slopes for both reactions increase with energy while the intercepts decrease. The difference of intercepts, however, shows a barely significant energy variation. At 7 GeV/c $\cos\phi_{VT} \propto (A_{K^-} - A_{\pi^+})/(A_{K^-} + A_{\pi^+})$ is 0.063 ± 0.067 whereas it is -0.021 ± 0.059 at 11.5 GeV/c. Exchange degeneracy predicts $\cos\phi_{VT} = 0$ and within errors this is satisfied at both energies. The 10 GeV/c data of Berglund et al.[2] show similar behavior for the differential cross sections, however, at larger momentum transfer small EXD violations are seen.

Strong EXD is ruled out at these energies by the non-zero polarizations (see Fig. 4c, d), however, the mirror polarizations for the line-reversed reactions support weak EXD. This simple reflection symmetry of the Σ polarization for this pair had not been seen before. In Fig. 5a, the 11.5 GeV/c data is again shown for the π^+ and K^- induced reactions together with the sum (Fig. 5b) of the polarization from the π^+ and the K^- reactions. The χ^2 for the hypothesis that all these points lie on the abscissa is 3.9 for 6 degrees of freedom.

The prediction of the model of Navelet and Stevens[7] is compared to the summed polarizations results in Fig. 5b. It is shown as the solid line on the figure and is in obvious disagreement with the experimental data.

Data on the reactions $\pi^+p \to K^+\Sigma^+$ and $\pi^+p \to K^+Y^{*+}(1385)$ have been reported using the Fermilab Single Arm Spectrometer Facility at 70 GeV/c.[3] For $-t < 0.1$ GeV^2 the $Y^*(1385)$ signal is much smaller than the Σ^+, whereas for larger t the two signals become comparable (see Fig. 6). Their results

show positive Σ^+ polarization, Fig. 7, which also rules out strong EXD at 70 GeV/c. The values appear to be more positive than the Navelet-Stevens[7] predictions, but very similar to the 7 and 11.5 GeV polarizations measured by SLAC-Imperial College.[8-10]

The Reactions $\pi^+p \to K^+Y^{*+}(1385)$ and $K^-p \to \pi^-Y^{*+}(1385)$

The polarization of the $Y^*(1385)$ is obtained by a combined maximum likelihood fit to the Y^* and Λ decay distributions in terms of the transversity density matrix elements. The results are shown in Fig. 8. In neither reaction is there any significant evidence for non-zero polarization. While this agrees with strong exchange degeneracy predictions, it is also predicted on the basis of the additive quark[11] and Stodolsky-Sakurai[12] models.

The differential cross sections are shown in Fig. 9. Both reactions have a turnover at low momentum transfer showing dominance of the helicity flip amplitude unlike Σ production. The line-reversed pair Y^* reactions show significant differences at small $|t|$, however, most of this difference is of kinematic origin: angular momentum conservation forces the two Y^* cross sections to turnover at different values of momentum transfer yielding different cross sections at small $|t|$.[10]

To describe this effect quantitatively, the SLAC group made fits to the differential cross sections using the function:

$$\frac{d\sigma}{dt} = \left[A_1 - A_2\,(t - t_{min})\right] e^{bt} \qquad (8)$$

where A_1 and A_2 approximate the helicity non-flip and flip contributions, respectively. The fits give a good description of the data as seen in

Fig. 9. The non-flip parameter A_1 is about 3% of the flip term A_2. The values of A_2 agree within errors for the line-reversed reactions giving confirmation of EXD predictions. They obtain at 11.5 GeV/c

$$\langle \cos \phi_{VT} \rangle = \frac{A_2(K^- p) - A_2(\pi^+ p)}{A_2(K^- p) + A_2(\pi^+ p)} = 0.05 \pm 0.10 \quad .$$

The only other experiment which has previously studied both pairs of reactions in a single experimental setup is a missing mass experiment at 10.1 GeV/c.[2] They found reactions (3) and (4) violated EXD predictions with a ratio of the $K^- p$ to $\pi^+ p$ cross sections of 2.0 ± 0.2 (see Fig. 10). In the same t-region the SLAC 11.5 GeV/c data gives a ratio of K^- to π^+ cross sections of 1.33 ± 0.14. In contrast, the two experiments agree on their results for the reactions $\pi^+ p \to K^+ \Sigma^+$ and $K^- p \to \pi^- \Sigma^+$.[2,10] The main difference between the two experiments is the amount of background in the region of the $Y^*(1385)$. In Fig. 11, the missing-mass-squared distributions for the two experiments are given. The SLAC experiment has very little background because they measure in the bubble chamber the other tracks and thereby enchance the signal from the $Y^*(1385)$ over background by topology and kinematic fitting. Since the Σ^+ signal is large, uncertainties in background subtraction are not as important.

Figure 12 shows the energy dependence of the $\pi^+ p \to K^+ \Sigma^+$ and $\pi^+ p \to K^+ Y^{*+}(1385)$ reactions at $t = -0.1$ GeV^2. We see a faster falloff for the Σ^+ than for the Y^* reaction. This means that other exchanges than the weak degenerate K^*_{890} and K^{**}_{1420} may be present.

Amplitude Analysis of $Y^*(1385)$ Production in the Line-Reversed Reactions: $\pi^+p \to K^+Y^*(1385)$ and $K^-p \to \pi^-Y^*(1385)$

The additive quark model assumes that peripheral interactions occur by a single quark-quark scattering process. Only in the single scattering process does quantum number exchange take place.

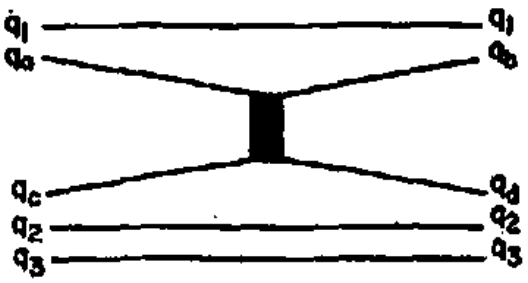

The spectator quarks recombine with the scattered quarks to form the final state hadrons. A single scattering process means baryon exchanges are not allowed and the small u-channel cross sections support this.

The OZI rule[13] is a direct consequence of this limitation. The reaction $\pi^-p \to \phi n$ is forbidden by this rule as well as $\pi^-p \to \psi n$. The $\phi(\psi)$ is mainly a state of $s\bar{s}(c\bar{c})$ quarks. In order for the reaction to take place two scattering processes would be required.

The predictions of the additive quark model for the correlati between the charge properties and spin configurations in peripheral collisions have been successfully tested in a number of reactions. The constraint that only one quark in each hedron interacts, places requirements on the allowed spin states of the final hadrons. One can also identify the quark-quark amplitudes in different reactions, then obtain relations between these reactions.

As an example, the reaction

$$K^- p \to \pi Y^{*++}(1385)$$

$$0^- \frac{1}{2}^+ \to 0^- \frac{3}{2}^+ \tag{9}$$

in general can have four independent amplitudes. If the quark model relations are satisfied only one amplitude remains. To see this we show in the diagram below the scattering process $K^- p \to \pi Y^*$.

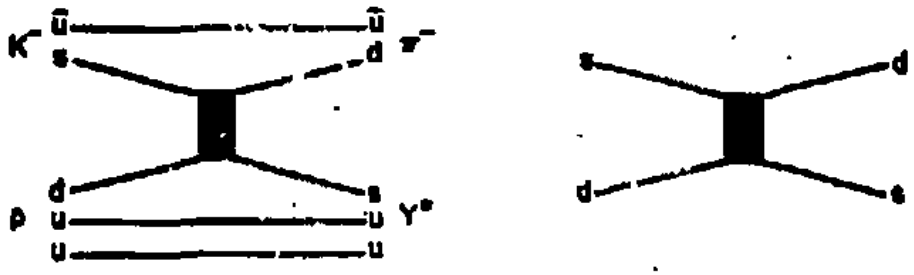

Here we see that the scattering process is $sd \to ds$ of spin 1/2 particles. We choose the axis of spin quantization in the direction normal to the quark-quark scattering plane. The spin projection on this axis is called the transversity.

The spin projection of a single quark can only change by zero or one unit along any axis. Therefore, a change of two or more units of angular momentum at any vertex, is forbidden. A transversity flip at the baryon vertex requires a flip in the opposite direction at the meson vertex to conserve transversity. Since the final state meson has spin 0^-, only transversity non-flip amplitudes are allowed by the additive quark model in reaction (9). This implies

$$T_{\frac{3}{2}-\frac{1}{2}} = T_{-\frac{3}{2}\frac{1}{2}} = 0$$

$$T_{\frac{1}{2}\frac{1}{2}} = T_{-\frac{1}{2}-\frac{1}{2}} \tag{10}$$

In this model, any double-flip amplitudes come from more than one scatter in the quark-quark scattering process.

SLAC and Imperial College[14] measure for the first time in one detector the complete decay angular distribution on $Y^* \to \Lambda\pi$, $\Lambda \to p\pi^-$ in the π^+p and K^-p line-reversed reactions. The results for the four measureable transversity amplitudes are shown in Fig. 13 together with the predictions of the additive quark model[11] and Stodolsky-Sakurai[12] models. In general, the data agree with these predictions. However, the only significant non-zero double-flip values are at small t similar to what has been observed at 4.2 GeV/c in K^-p interactions.[6] In the quark model described above, these double-flip contributions imply double quark scattering processes. This effect also may be associated with a finite helicity non-flip contribution to the $Y^*(1385)$ vertex. At $t = t_{min}$, all helicity flip amplitudes go to zero and any remaining non-flip contributions forces the transversity amplitudes to the values:

$$\left|T_{\pm\frac{3}{2}\pm\frac{1}{2}}\right| = \sqrt{\frac{3}{8}} \qquad \left|T_{\pm\frac{1}{2}\pm\frac{1}{2}}\right| = \sqrt{\frac{1}{8}}$$

The trend of the data is in qualitative agreement with these values.

Conclusions

In contrast to the lower energy data, the 11.5 GeV results for the two pairs of line-reversed, hypercharge-exchange reactions are consistent with exchange degeneracy predictions for both helicity-flip and non-flip amplitudes.

The $Y^*(1385)$ decay angular distributions indicate that the quark model and Stodolsky-Sakurai predictions are in agreement with the main

features of the data. However, small violations are observed at small momentum transfer. While the $Y^*(1385)$ vertex is helicity-flip dominated, the non-vanishing of $T_{3/2-1/2}$ and $T_{-3/2\ 1/2}$ suggests some finite helicity non-flip contribution in the forward direction.

Acknowledgements

I wish to thank the Organizing Committee for their kind hospitality. My special thanks goes to Patricia Dorflinger for the typing of this manuscript. The helpful discussions and comments of my colleagues in Experimental Group BC at SLAC are appreciated.

References

1) K.-W. Lai and J. Louie, Nucl. Phys. B19, 205 (1970).

2) A. Berglund et al., Phys. Lett. 60B, 117 (1975), and
A. Berglund et al., Phys. Lett. 73B, 369 (1978).

3) M. W. Arenton et al., "Measurement of Exclusive Hypercharge-Exchange Reactions at 35 to 140 GeV/c," ANL-HEP-PR-78-24.

4) G. B. Bowden et al., Nucl. Instr. Methods 138, 75 (1976),
J. Ballam and R. Watt, Ann. Rev. Nucl. Sci. 27, 75 (1977),
R. C. Field, Stanford Linear Accelerator Center, Internal Publication, SHF Memo 67, Group BC (1977).

5) M. Aderholz et al., Nucl. Phys. B11, 259 (1969),
A. Baehian et al., Phys. Rev. D 4, 2667 (1971),
M. Aguilar-Benitez et al., Phys. Rev. D 6, 29 (1972),
D. Birnbaum et al., Phys. Lett. 31B, 484 (1970),
B. Chaurand et al., Nucl. Phys. B117, 1 (1976).

6) S. O. Holmgren et al., Nucl. Phys. B119, 261 (1977).

7) H. Navelet and P. R. Stevens, Nucl. Phys. B104, 171 (1976).

8) P. A. Baker et al., "Experimental Test of Exchange Degeneracy in Hypercharge Exchange Reactions at 7 and 11.5 GeV/c", Stanford Linear Accelerator Center preprint SLAC-PUB-2169 (1978).

9) P. A. Baker et al., Phys. Rev. Lett. 40, 678 (1978).

10) J. Ballam et al., Phys. Rev. Lett. 41, 676 (1978).

11) A. Bialas and K. Zalewski, Nucl. Phys. B6, 449 (1968).

12) L. Stodolsky and J. J. Sakurai, Phys. Rev. Lett. 11, 90 (1963).

13) S. Okubo, Phys. Lett. 5, 165 (1963); G. Zweig, CERN preprint TH-412 (1964); J. Iizuka, K. Okada, and O. Shito, Prog. Theoret. Phys. 35, 1061 (1966); J. Iizuka, Suppl. of Prog. Theoret. Phys. 37-38, 21 (1966).

14) J. Ballam et al., "Amplitude Analysis of $Y^*(1385)$ Production in the Line-Reversed Reactions: $\pi^+p \to K^+Y^*(1385)$ and $K^-p \to \pi^-Y^*(1385)$ at 7 and 11.5 GeV/c," Stanford Linear Accelerator Center preprint SLAC-PUB-2175 (1978).

Figures

1) Missing-mass-squared distribution for π^+ in the beam and K^+ in the spectrometer, summed over all 70 GeV/c data. Figure from Ref. 3.

2) Perspective drawing of the SLAC Hybrid Facility. The cylindrical bubble chamber is represented in a cut-away drawing of its magnet body. Steel hadron filters are indicated before S4 and S5.

3) Invariant mass distribution of the $\Lambda\pi^+$ system at 11.5 GeV/c. Figure from Ref. 8.

4) Differential cross sections and Σ polarizations for the reactions $\pi^+p \to K^+\Sigma^+$ and $K^-p \to \pi^-\Sigma^+$ at 7 and 11.5 GeV/c. Figure from Ref. 8.

5) a) Σ^+ polarization for the SLAC 11.5 GeV data.

b) Sum of the polarizations for the π^+ and K^- reactions. The curve is the prediction of the model of Navelet and Stevens (Ref. 7) as described in the text.

6) Preliminary differential cross section at 70 GeV/c for the reactions $\pi^+p \to K^+\Sigma^+$ and $\pi^+p \to K^+Y^{*+}(1385)$. Data from Ref. 3.

7) Preliminary results on the polarization of the recoil Σ^+. The curve is the prediction at 70 GeV/c of Navelet-Stevens.[7] Data from Ref. 3 and Ref. 8.

8) $Y^*(1385)$ polarization at 11.5 GeV/c.

9) Differential cross sections and $\cos\phi_{VT} = \left[\frac{d\sigma}{dt}(K^-p) - \frac{d\sigma}{dt}(\pi^+p)\right] \Big/ \left[\frac{d\sigma}{dt}(K^-p) + \frac{d\sigma}{dt}(\pi^+p)\right]$ for $\pi^+p \to K^+Y^*(1385)$ and $K^-p \to \pi^-Y^*(1385)$ at 11.5 GeV/c. Figure from Ref. 10.

10) Differential cross sections and $R = \frac{d\sigma}{dt}(K^-p) \Big/ \frac{d\sigma}{dt}(\pi^+p)$. (Note $\cos\phi_{VT} = \frac{R-1}{R+1}$ and $R = 2 \to \cos\phi_{VT} = 1/3$.) 10.1 GeV/c data from Berglund et al. Figure from Ref. 2 (1975).

11) Missing-mass-squared distributions for $\pi^+p \to K^+$ MM.

a) Berglund et al. at 10.1 GeV/c, Ref. 2.

b) SLAC 11.5 GeV/c data from Ref. 10 for the reaction $\pi^+p \to K^+\Lambda\pi^+$.

12) Dependence on P_{lab} of the Σ and $Y^*(1385)$ production at $t = 0.1$ GeV/c Data from Refs. 2, 3, and 8.

13) Absolute values of the $Y^*(1385)$ transversity amplitudes as a function of momentum transfer. The dashed lines are predictions of the additive quark model[11] and the model of Stodolsky-Sakurai.[12] Figure from Ref. 14.

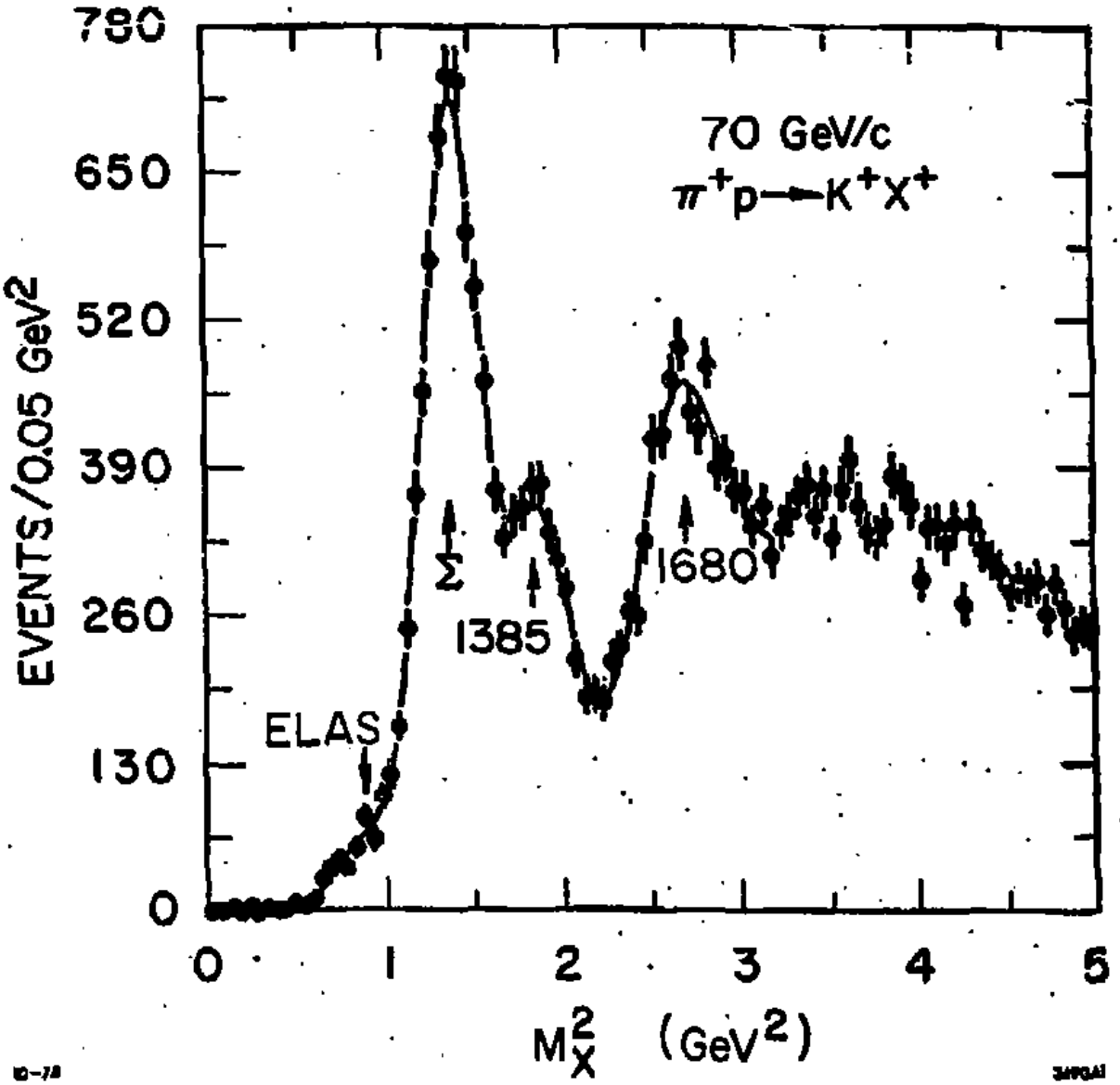
780
650
520
390
260
130
0
EVENTS/0.05 GeV2
70 GeV/c
π+p→K+X+
ELAS
M
1385
1680
0
1
2
3
4
5
M2X (GeV2)

Fig. 1

SLAC HYBRID FACILITY

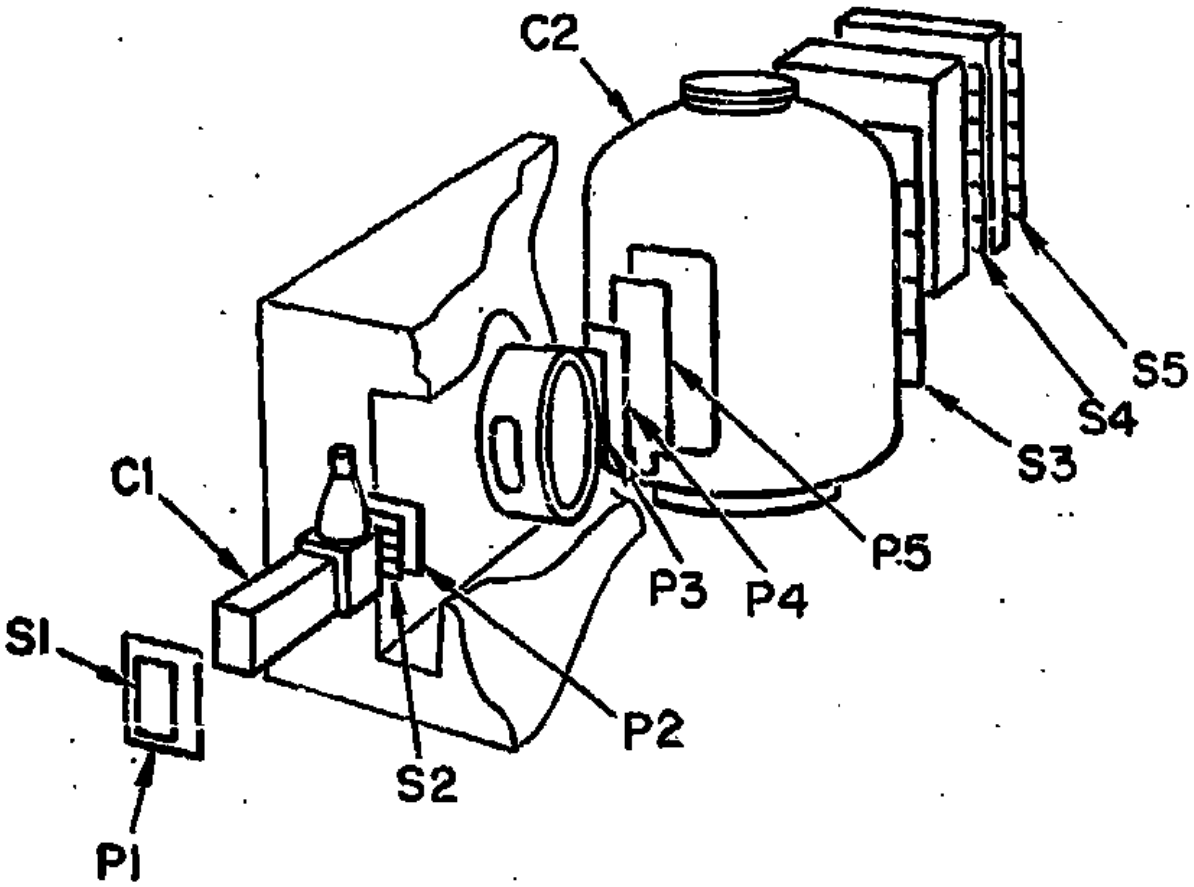

S1 Beam Scintillator
S2-5 Hodoscopes
C1-2 Cerenkov Counters
P1-5 P.W.C.s

9-78 3460A7

Fig. 2

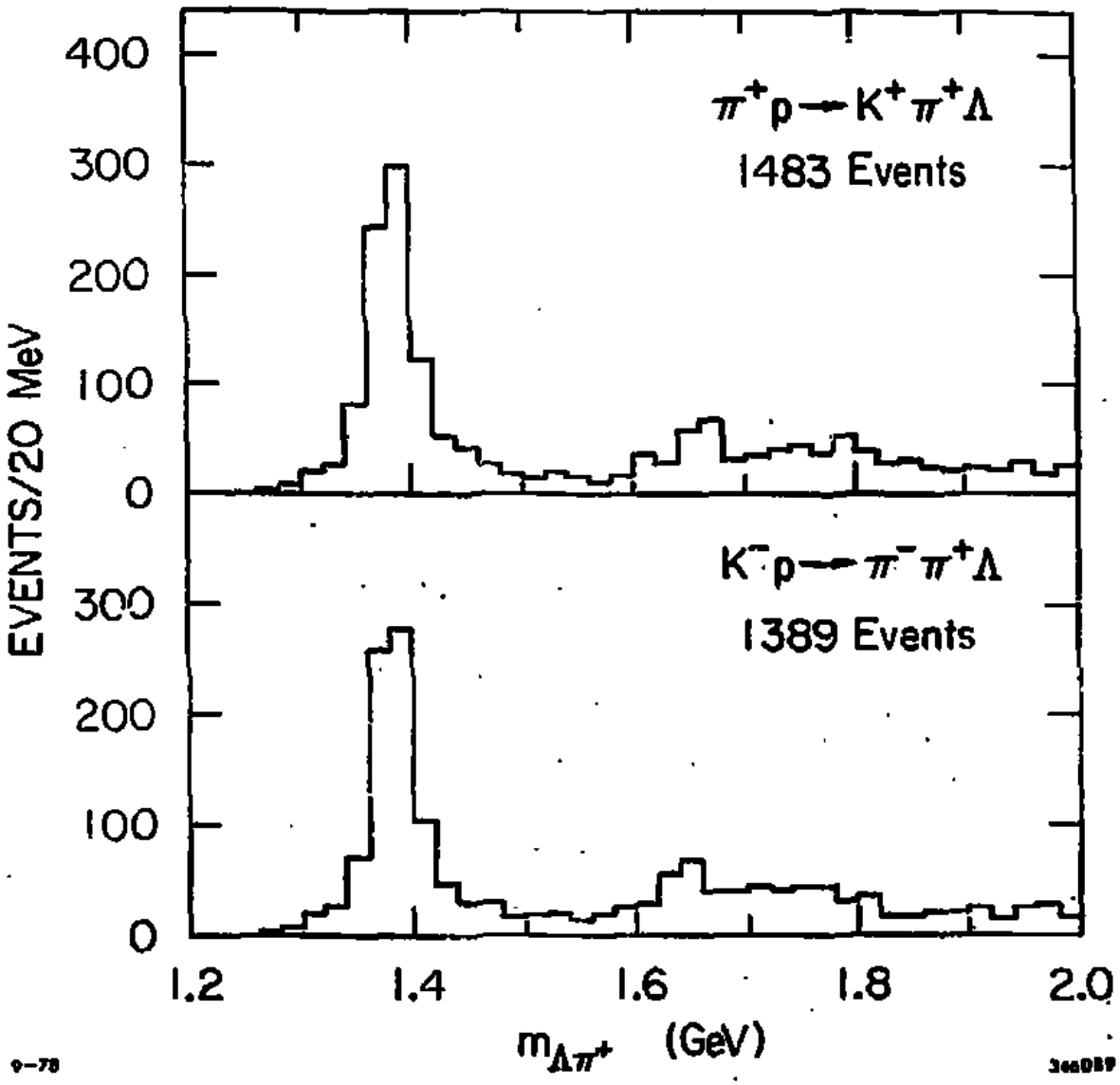
400
300
200
100
0
$\pi^+ p \rightarrow K^+ \pi^+ \Lambda$
1483 Events
300
200
100
0
$K^- p \rightarrow \pi^- \pi^+ \Lambda$
1389 Events
EVENTS/20 MeV
1.2
1.4
1.6
1.8
2.0
$m_{\Lambda\pi^+}$ (GeV)

Fig. 3

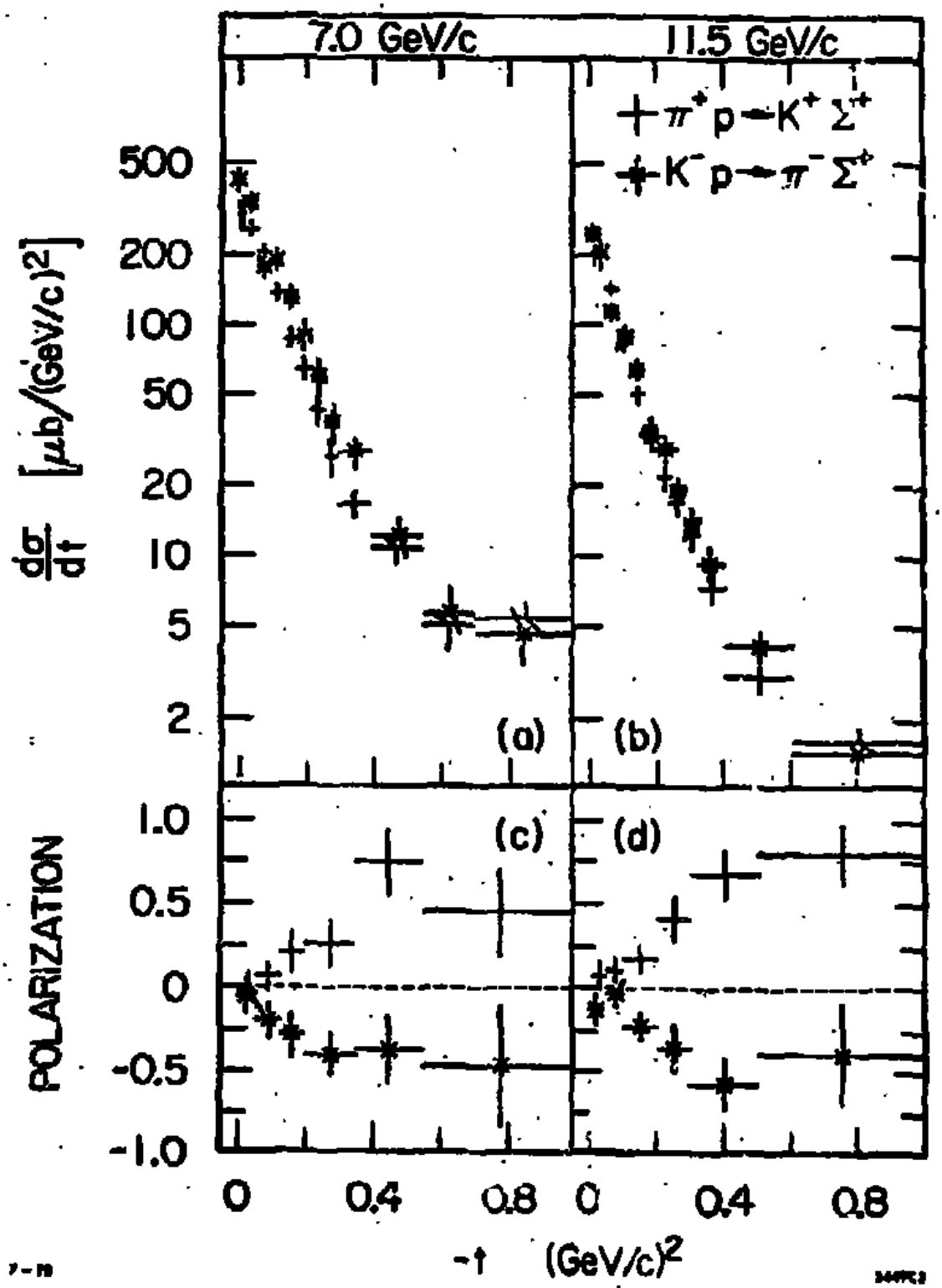
7.0 GeV/c
11.5 GeV/c
$\pi^+ p \to K^+ \Sigma^+$
$K^- p \to \pi^- \Sigma^+$
$\frac{d\sigma}{dt}$ [μb/(GeV/c)^2]
500
200
100
50
20
10
5
2
(a)
(b)
(c)
(d)
POLARIZATION
1.0
0.5
0
-0.5
-1.0
0
0.4
0.8
0
0.4
0.8
$-t$ (GeV/c)^2

Fig. 4

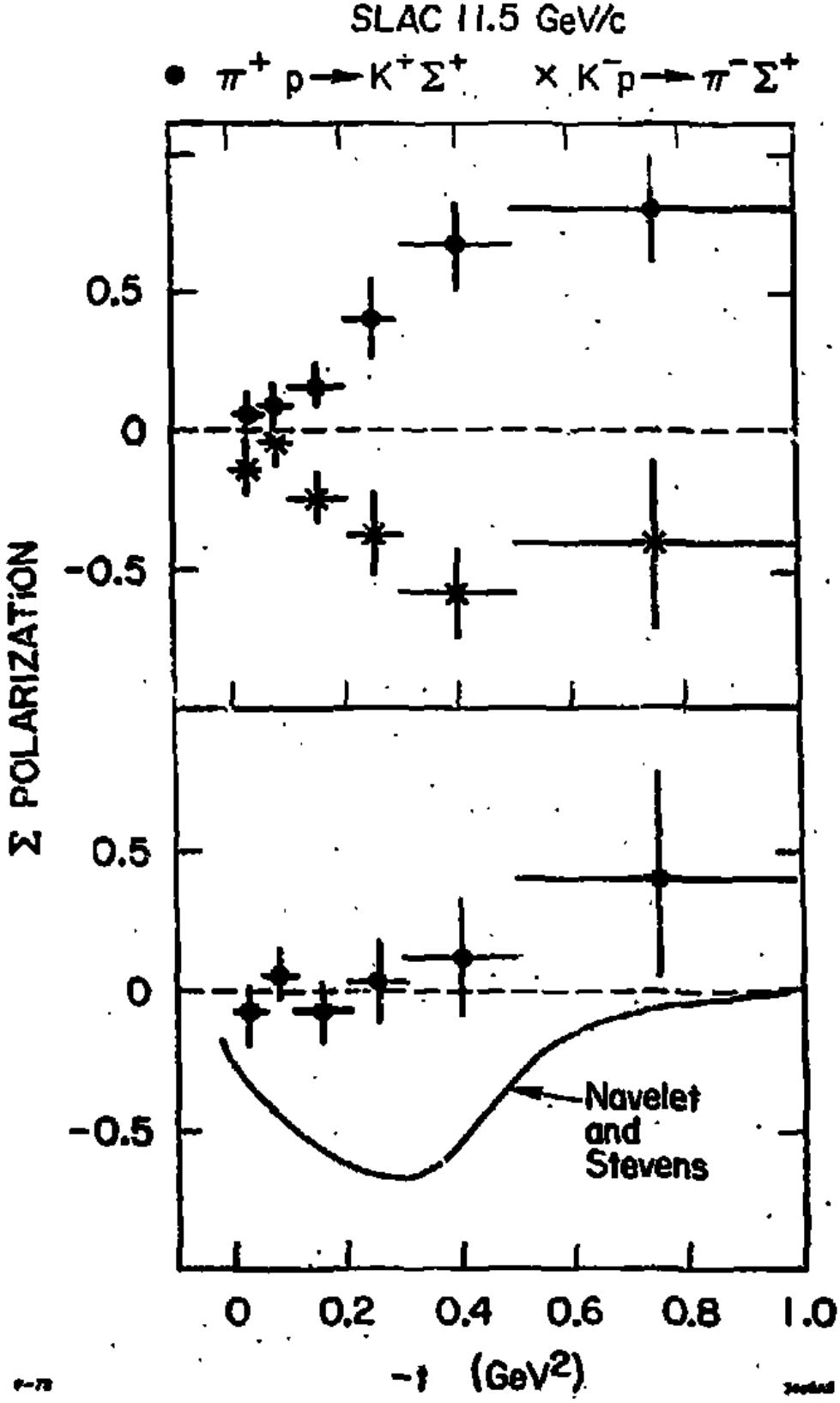
SLAC 11.5 GeV/c
● $\pi^+ p \rightarrow K^+ \Sigma^+$ × $K^- p \rightarrow \pi^- \Sigma^+$
Σ POLARIZATION
0.5
0
-0.5
0.5
0
-0.5
Navelet and Stevens
0
0.2
0.4
0.6
0.8
1.0
$-t$ (GeV^2)

Fig. 5

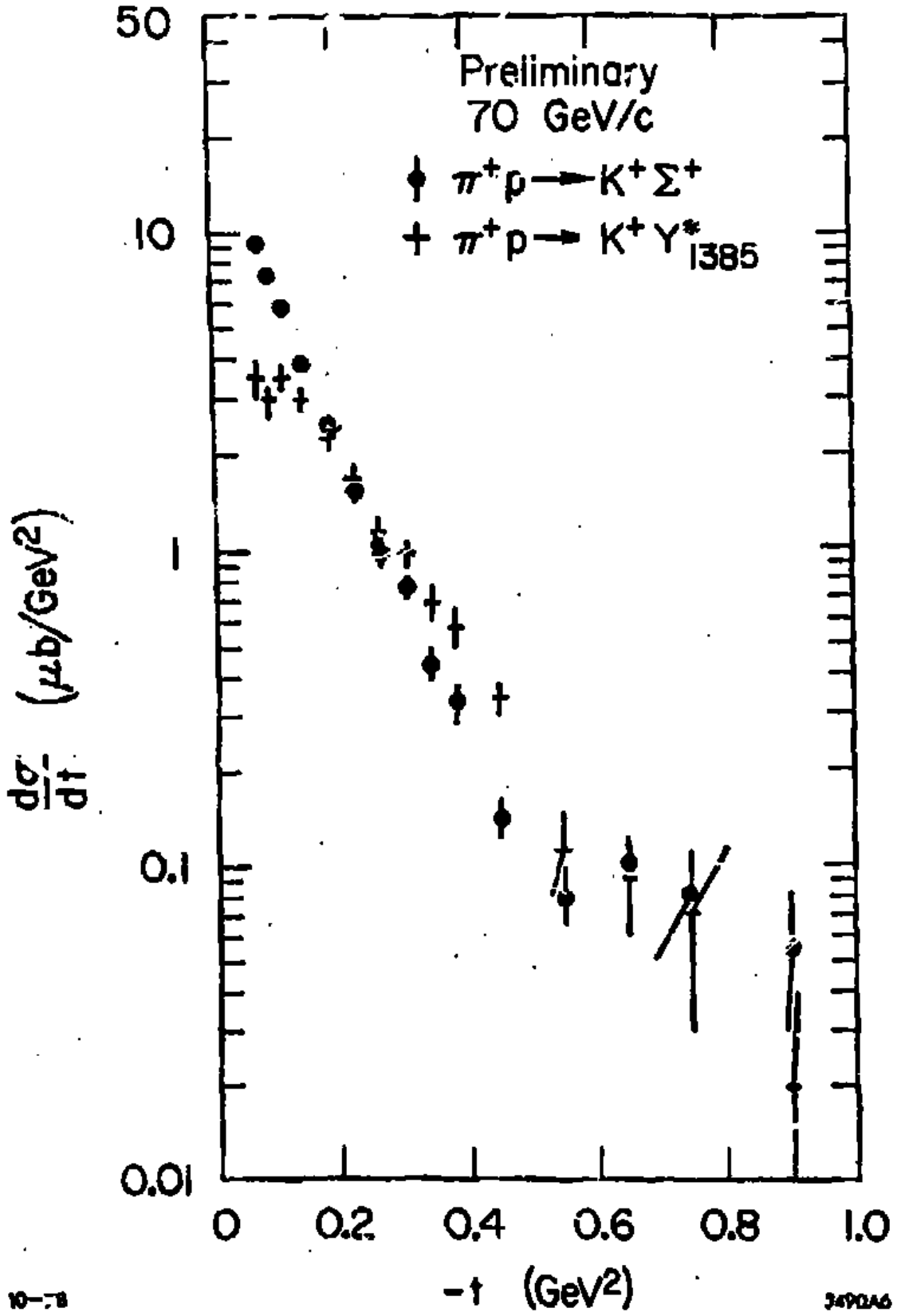
Preliminary
70 GeV/c
π⁺p → K⁺Σ⁺
π⁺p → K⁺Y*1385
50
10
1
0.1
0.01
dσ/dt (μb/GeV²)
0
0.2
0.4
0.6
0.8
1.0
-t (GeV²)
10-78
3490A6

Fig. 6

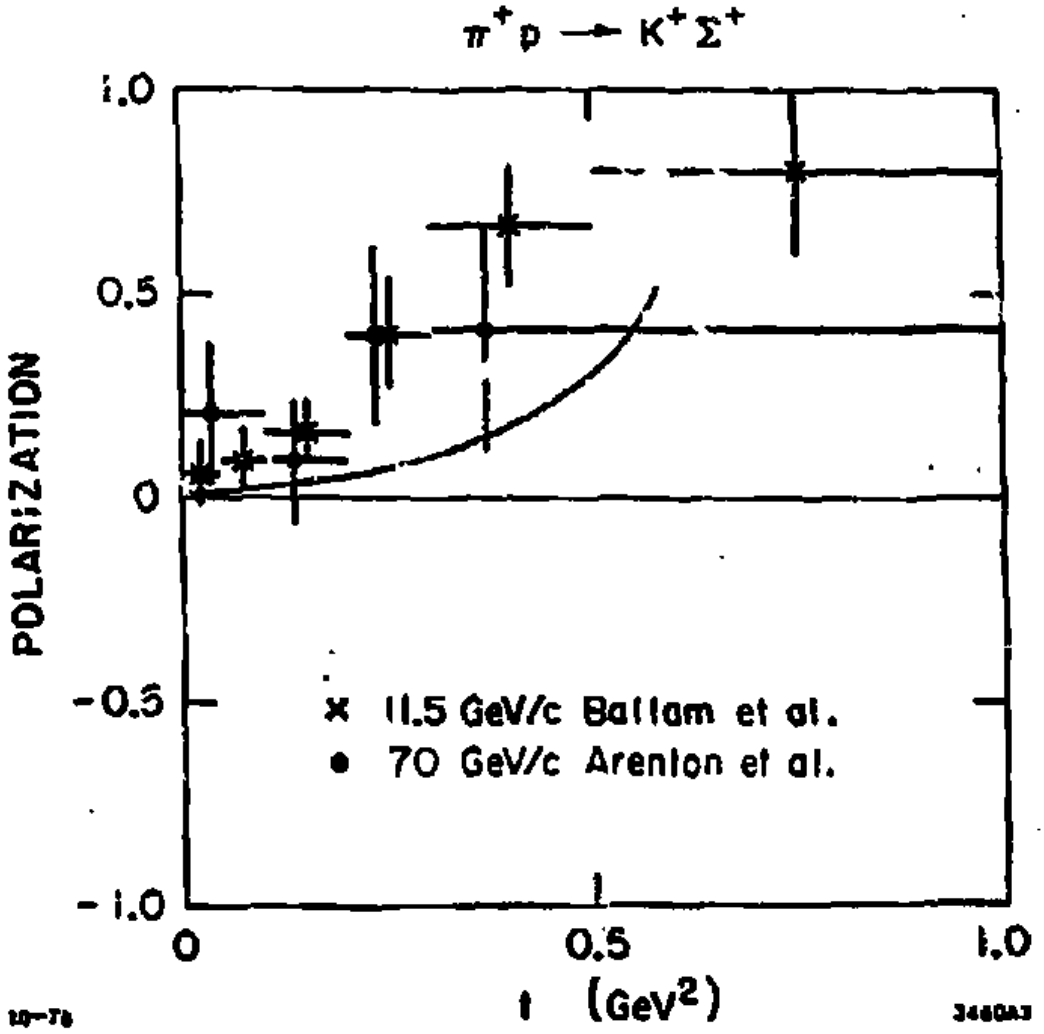
$\pi^+ p \rightarrow K^+ \Sigma^+$
1.0
0.5
0
-0.5
-1.0
POLARIZATION
× 11.5 GeV/c Baltam et al.
• 70 GeV/c Arenton et al.
0
0.5
1.0
t (GeV²)

Fig. 7

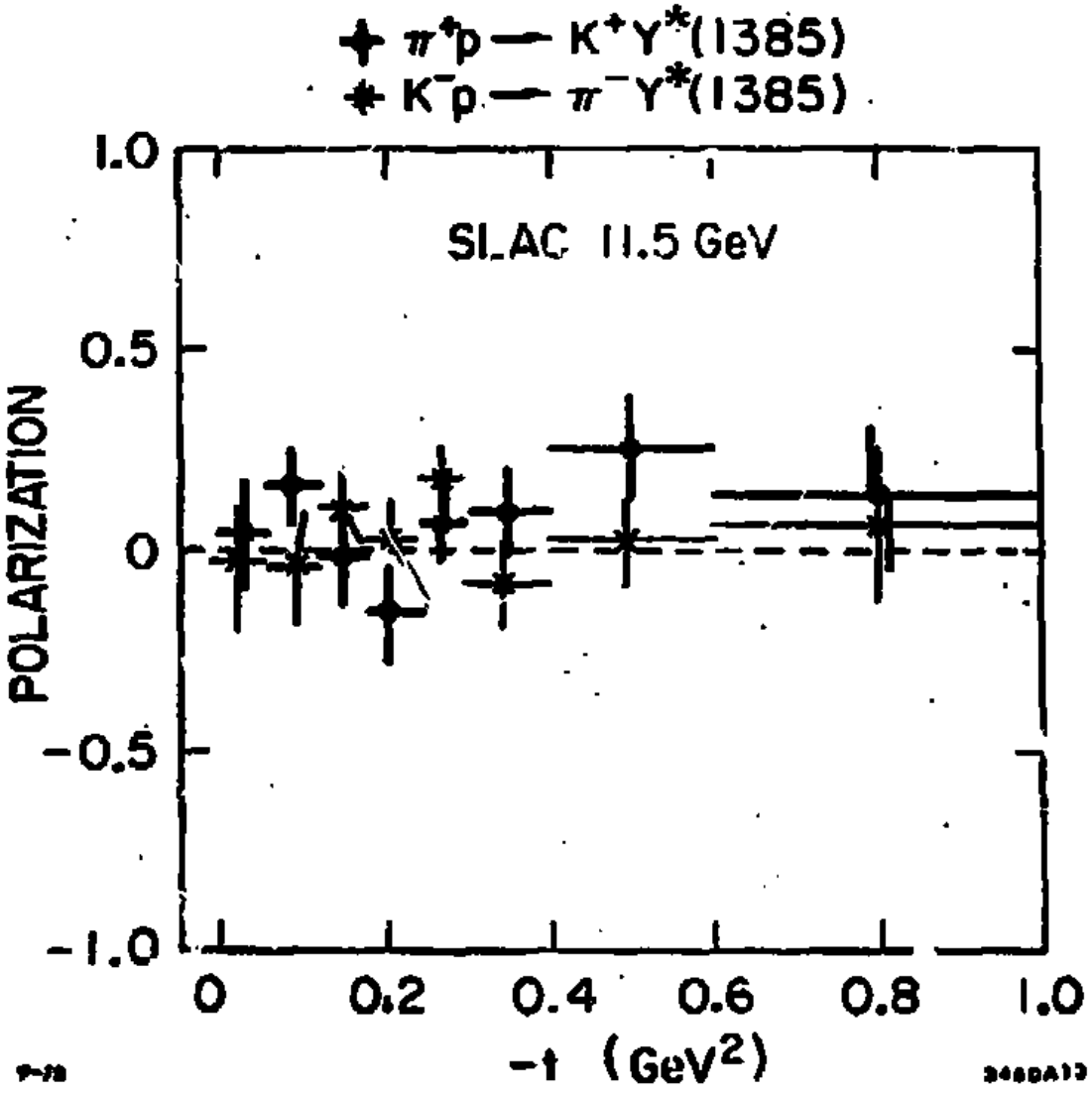
$\pi^+ p \rightarrow K^+ Y^*(1385)$
$K^- p \rightarrow \pi^- Y^*(1385)$
SLAC 11.5 GeV
POLARIZATION
1.0
0.5
0
-0.5
-1.0
0
0.2
0.4
0.6
0.8
1.0
$-t$ (GeV^2)

Fig. 8

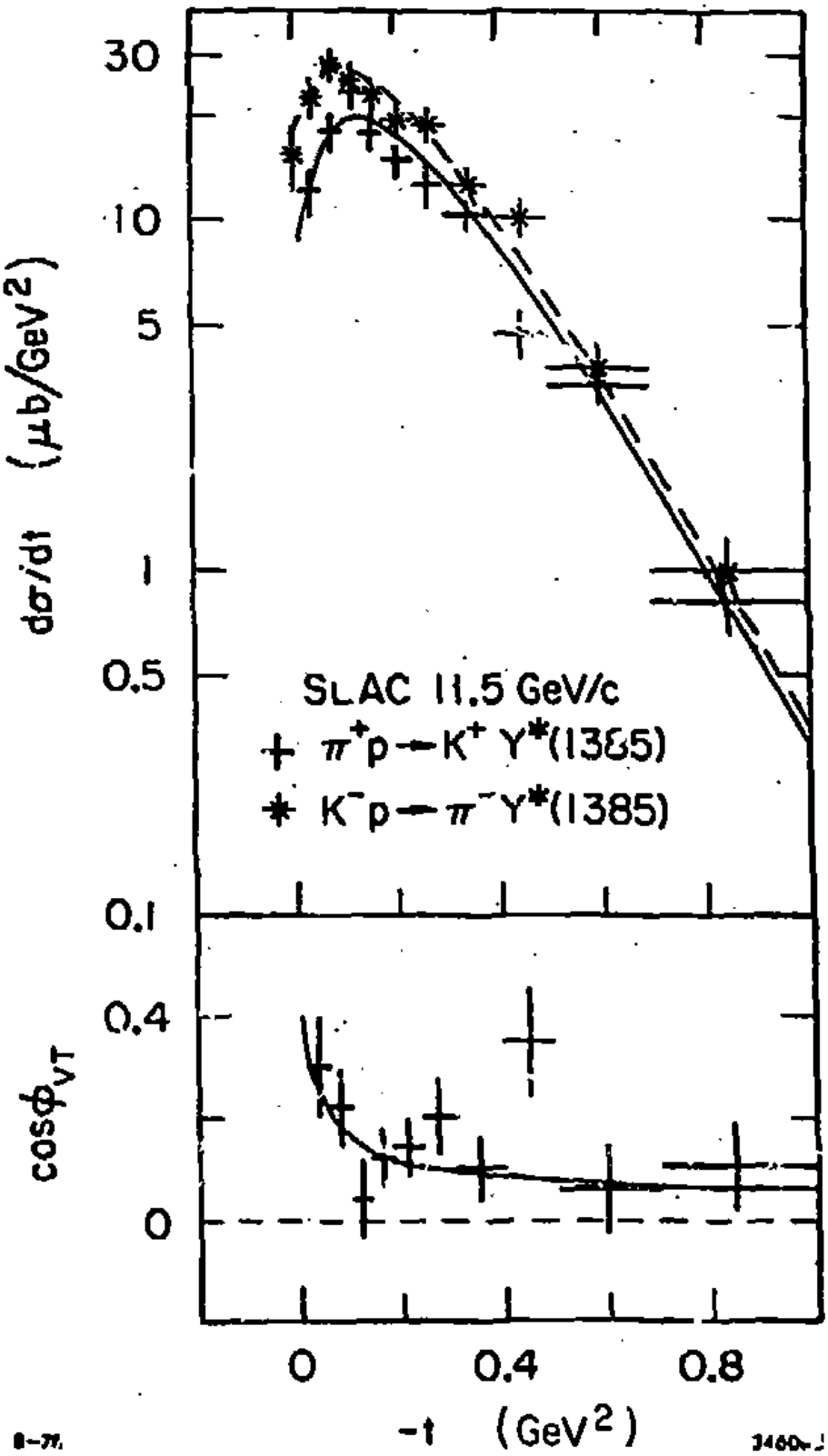
30
10
5
1
0.5
0.1
dσ/dt (μb/GeV²)
SLAC 11.5 GeV/c
+ π⁺p → K⁺ Y*(1385)
* K⁻p → π⁻ Y*(1385)
0.4
0
cosφ_VT
0
0.4
0.8
-t (GeV²)

Fig. 9

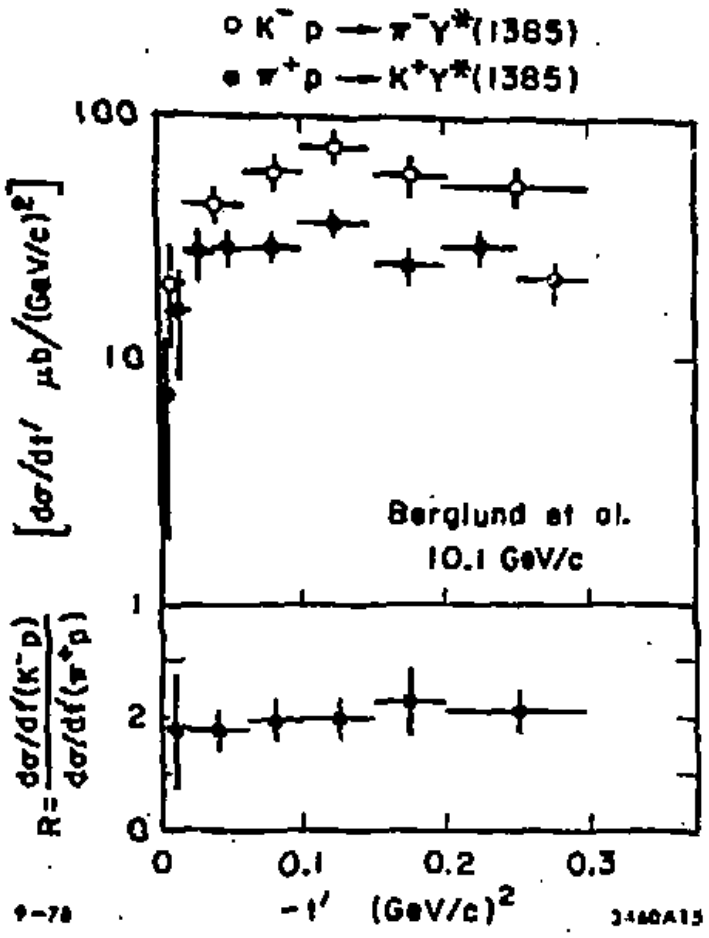
o K⁻ p → π⁻Y*(1385)
• π⁺ p → K⁺Y*(1385)
100
10
1
2
0
[dσ/dt' μb/(GeV/c)²]
R = dσ/dt'(K⁻p) / dσ/dt'(π⁺p)
Berglund et al.
10.1 GeV/c
0
0.1
0.2
0.3
-t' (GeV/c)²
9-78
3460A15

Fig. 10

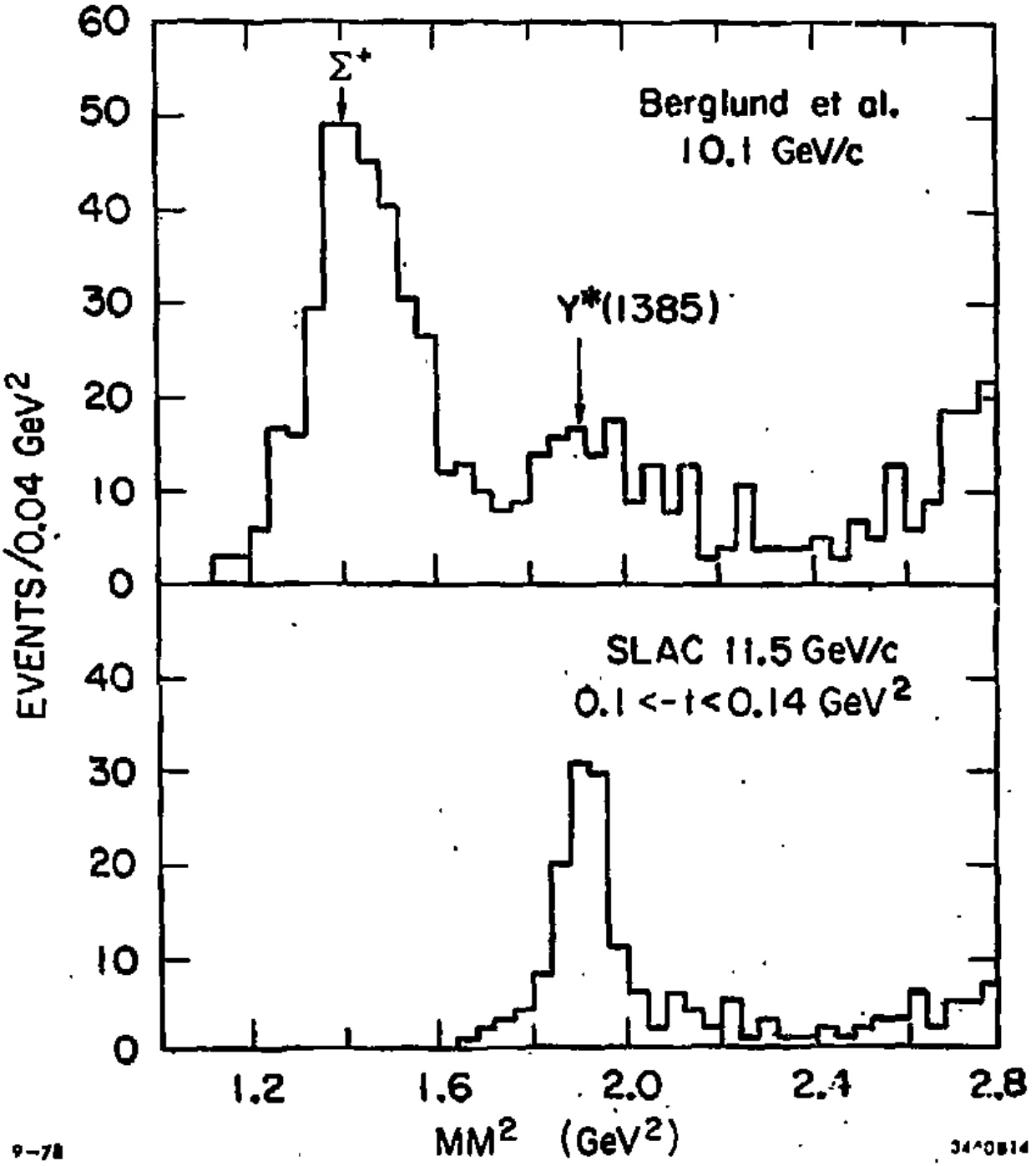
Σ+
Berglund et al.
10.1 GeV/c
Y*(1385)
SLAC 11.5 GeV/c
0.1 <-t<0.14 GeV²
EVENTS/0.04 GeV²
MM² (GeV²)
60
50
40
30
20
10
0
40
30
20
10
0
1.2
1.6
2.0
2.4
2.8
9-78
3440814

Fig. 11

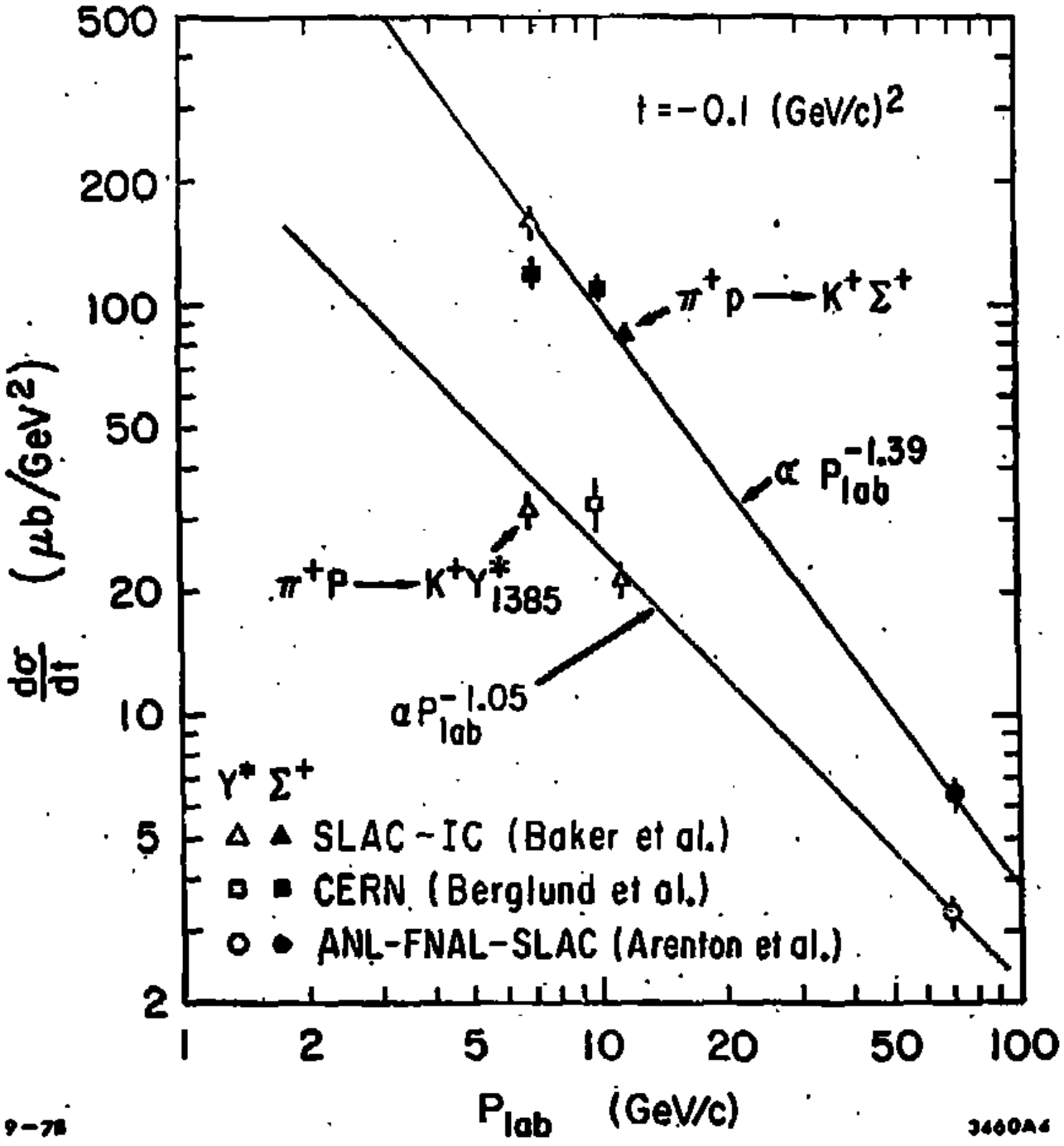
500
200
100
50
20
10
5
2
1
2
5
10
20
50
100
t = −0.1 (GeV/c)²
π⁺p → K⁺Σ⁺
α P_lab^−1.39
π⁺p → K⁺Y*1385
α P_lab^−1.05
Y* Σ⁺
SLAC-IC (Baker et al.)
CERN (Berglund et al.)
ANL-FNAL-SLAC (Arenton et al.)
dσ/dt (μb/GeV²)
P_lab (GeV/c)
9-78
3460A4

Fig. 12

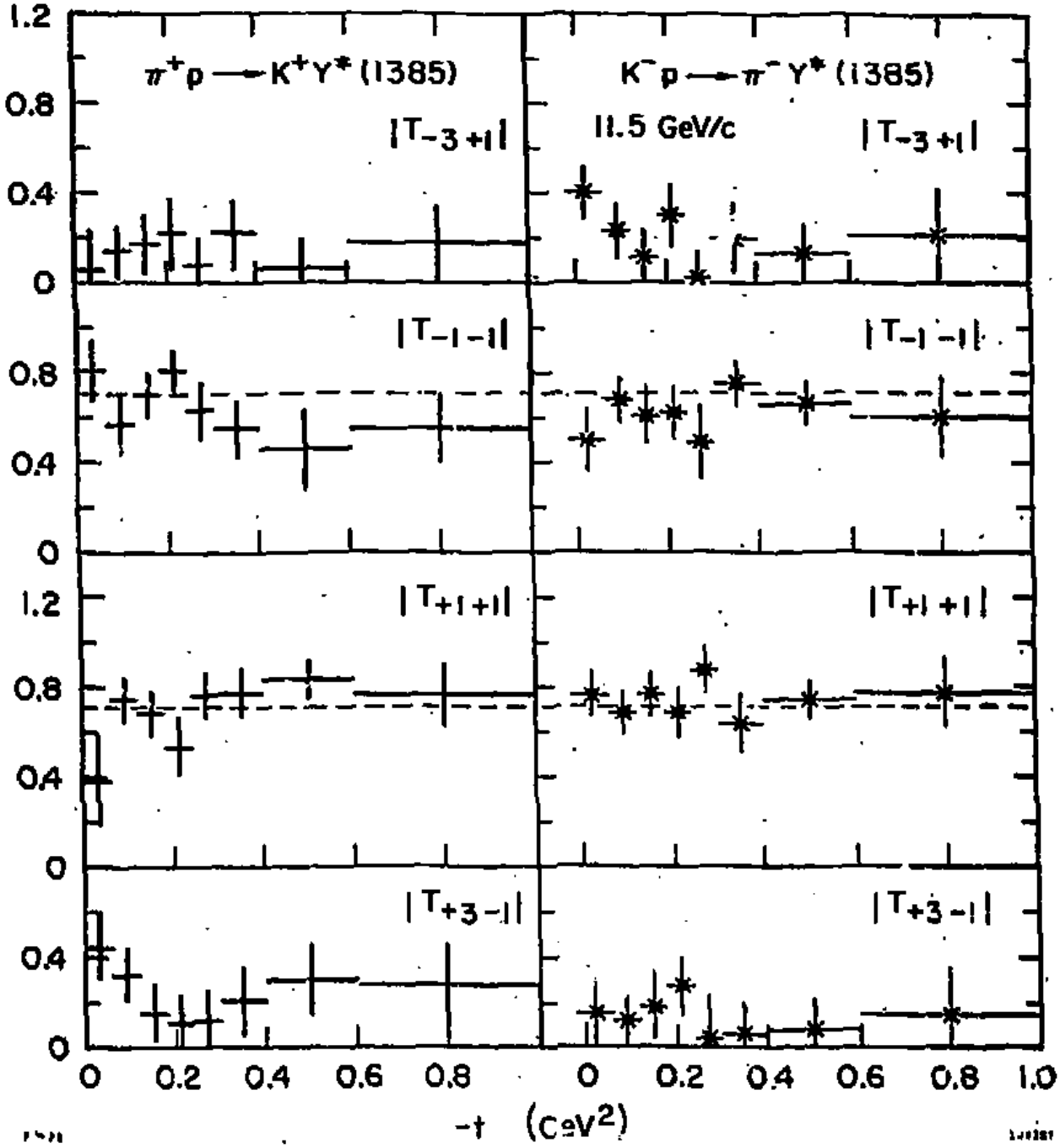
$\pi^+ p \rightarrow K^+ Y^*(1385)$
$K^- p \rightarrow \pi^- Y^*(1385)$
11.5 GeV/c
$|T_{-3+1}|$
$|T_{-1-1}|$
$|T_{+1+1}|$
$|T_{+3-1}|$
1.2
0.8
0.4
0
0.2
0.6
1.0
$-t$ (GeV^2)

Fig. 13